Solar optics-based active panel for solar energy storage and disinfection of greywater

W. Lee,[1] J. Song,[1,2] J. H. Son,[2] M. P. Gutierrez,[3] T. Kang,[4,a)] D. Kim,[1,a)] and L. P. Lee[2,a)]

[1]*Department of Mechanical Engineering, Sogang University, 04107 Seoul, South Korea*
[2]*Departments of Bioengineering, Electrical Engineering and Computer Science, and Biophysics Program, University of California, Berkeley, California 94270, USA*
[3]*Department of Architecture, University of California, Berkeley, California 94270, USA*
[4]*Department of Chemical and Biomolecular Engineering, Sogang University, 04107 Seoul, South Korea*

(Received 21 June 2016; accepted 10 October 2016; published online 24 October 2016)

Smart city and innovative building strategies are becoming increasingly more necessary because advancing a sustainable building system is regarded as a promising solution to overcome the depleting water and energy. However, current sustainable building systems mainly focus on energy saving and miss a holistic integration of water regeneration and energy generation. Here, we present a theoretical study of a solar optics-based active panel (SOAP) that enables both solar energy storage and photothermal disinfection of greywater simultaneously. Solar collector efficiency of energy storage and disinfection rate of greywater have been investigated. Due to the light focusing by microlens, the solar collector efficiency is enhanced from 25% to 65%, compared to that without the microlens. The simulation of greywater sterilization shows that 100% disinfection can be accomplished by our SOAP for different types of bacteria including *Escherichia coli*. Numerical simulation reveals that our SOAP as a *lab-on-a-wall* system can resolve the water and energy problem in future sustainable building systems. *Published by AIP Publishing*. [http://dx.doi.org/10.1063/1.4965855]

I. INTRODUCTION

Depleting energy sources and water have begun to threaten the sustainability of human in future.[1–3] It was expected that 2.8 billion people in 48 countries will suffer from water scarcity in 2025.[3] Nonetheless, regenerable greywater that accrues from 40%–70% of the total wastewater production in residential (e.g., bathroom sinks, bathtubs, and laundry) is still being wasted.[4,5]

To this end, several systems have been developed to utilize solar radiation for applications of greywater reuse[6–9] and solar energy storage[10–19] aiming emerging demands towards establishing NetZero waste, energy, and water buildings.[20–23] The disinfection of greywater by the solar radiation can be categorized according to the heating effect and the photoinactivation effect by the solar radiation. For example, the heating effect of solar radiation can be achieved with the optical concentration devices (e.g., lens and mirror) and it increases the temperature of water in order to complete inactivation of *Escherichia coli* in the greywater.[6] Similarly, the photoinactivation effect can be achieved by exposing the greywater on ultraviolet solar radiation without any optical concentration devices.[7–9] The solar energy storages can be accomplished by the absorbing solar radiation. For instance, most of the solar energy storage store the solar radiation by using a black surface[10,11] or nanofluid (nanoparticles in a liquid)[12–14] as absorbers. Optical concentration devices also ensure high solar radiative fluxes with relatively low thermal losses.[15,16] The stored solar energy is converted to electricity by using the

[a)]Authors to whom correspondence should be addressed. Electronic addresses: twkang@sogang.ac.kr; dckim@sogang.ac.kr; and lplee@berkeley.edu

thermoelectric converter[17] or directly used for radiant floor heating in buildings.[18,19] However, current designs of solar optics-based systems are focused on the generation of energy separately from the regeneration of water and the processing of waste. For example, the greywater reuse system has only focused on the solar disinfection function without the solar energy harvesting. The systems for radiant floor heating and solar energy storage have not included the function of regeneration of water.

Advanced solar optics-based systems, which can integrate solar energy storage component and solar thermal disinfection function, offer transformative benefits for advancing the growing challenges of water, energy, and waste in buildings.[24,25] Such systems can enable water conservation, on-site waste processing, and energy generation fomenting healthy environments and synergies with nature.

Here, we present a theoretical study of an innovative sustainable *lab-on-a-wall* system called solar optics-based active panel (SOAP),[25] which has dual functions of solar energy storage and photothermal disinfection of bacteria in greywater. Additionally, our SOAP can achieve the disinfection in a few minutes and can store the energy without any additional energy storage materials because the greywater is used as a thermal energy storage material. Our SOAP design consists of an optical microlens array on top of fluidic channels. The effects of SOAP's geometry (e.g., ratio of the optical lens diameter to the fluidic channel width and flow rate) and regional climate conditions with regards to solar energy storage and thermal disinfection efficiency are systematically evaluated.

II. RESULTS AND DISCUSSIONS

A. Design of SOAP

Our design of SOAP can be installed on the facades of buildings where a greywater collection and recirculation system are demanded (Figure 1). Once the greywater is collected (decentralized—floor to floor), it is housed through the SOAP panel in building facades, where

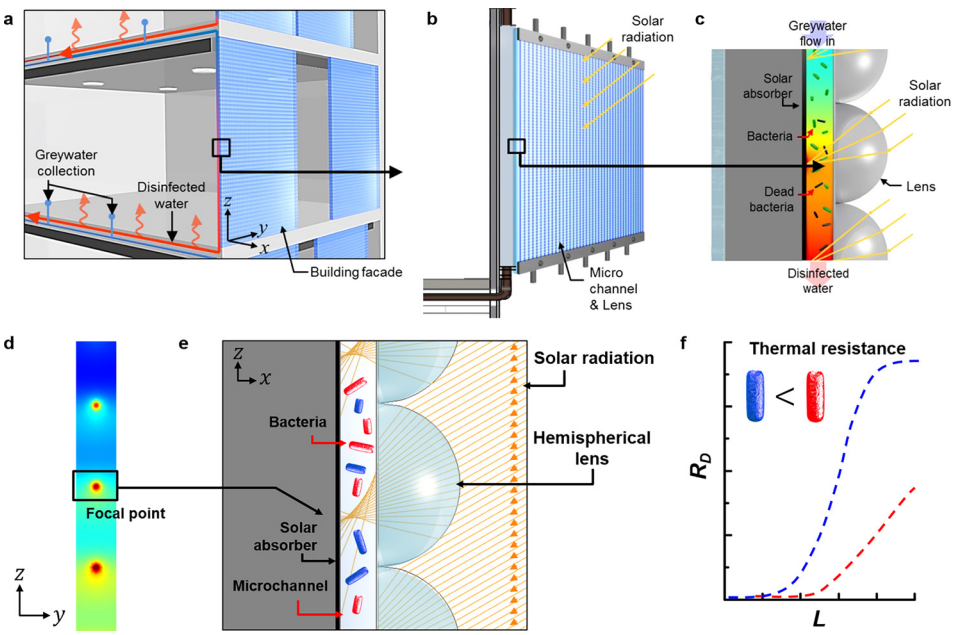

FIG. 1. Solar Optic-based Active Panel (SOAP), a holistic integration of water regeneration and energy storage: (a) Greywater collection and recirculation system in sustainable building with SOAP. (b) SOAP on the building facade to harness solar radiation for solar energy storage and thermal disinfection. (c) Detailed SOAP design consisting of optical lens array on top of microfluidic channels where greywater is housed. (d) Temperature field at the bottom along the microchannel. (e) Representative image of concentrated solar radiation on SOAP. (f) Disinfection of bacteria depending on their thermal resistance. R_D and L represent the disinfection rate and distance from the inlet, respectively.

photothermal disinfection of bacteria according to their thermal resistance can be achieved by utilizing optical lens for focusing solar radiation on the fluidic channel. Subsequently, the disinfected water is recirculated within each building floor for thermal radiation (hydronics) with or without a heat exchange (dependent on water temperature) into the building for reuse in toilet flushing and/or laundry.

B. Methods

In order to investigate the effect of geometry on SOAP's design, numerical simulations are performed by using commercial multiphysics software (COMSOL Multiphysics 4.4; COMSOL, Inc.). A local fluid velocity within the channels is required to investigate the change of water temperature under a continuous flow field. In order to calculate the local fluid velocity, the Navier–Stokes and continuity equations are solved, assuming that the flow is laminar and steady-state

$$\rho(\boldsymbol{u}\cdot\nabla)\boldsymbol{u} = -\nabla p + \mu\nabla^2\boldsymbol{u} - \frac{2}{3}\mu\nabla(\nabla\cdot\boldsymbol{u}), \tag{1}$$

$$\nabla\cdot(\rho\boldsymbol{u}) = 0, \tag{2}$$

where ρ, μ, p, and $\boldsymbol{u}$ represent the density, dynamic viscosity, pressure, and velocity vectors, respectively. We assumed the flow is laminar because the Reynolds number in our SOAP design is less than 10. The heat transfer in the SOAP system is calculated by considering conduction and convection

$$\rho c_p\boldsymbol{u}\cdot\nabla T = \nabla\cdot(k\nabla T) + Q, \tag{3}$$

where ρ, c_p, k, T, and Q stand for the density, specific heat of the water, thermal conductivity, temperature, and heat source, respectively. In order to calculate the heat loss on the exterior surface of the SOAP panel, we apply natural convective heat flux modeled as being proportional to the temperature difference across the surface (see supplementary material for the detailed simulation).

C. Solar energy storage

Figure 2(a) shows the effect of the optical lens array on the average temperature of water with respect to a mass flow rate and their corresponding schematic images. Installation of the optical lens array on top of the SOAP channels enables SOAP to overcome the limitations on the temperature of water in the channels without the optical lens array. Without the lens, the average temperature of water is calculated to be increased from 20 °C at the inlet of the channel to about 57 °C at the outlet of the channel irrespective of the given mass flow rate ranging from 10^{-6} to 10^{-8} kg/s. However, with the optical lens array on top of the SOAP channels, the temperature is increased to between 75 °C and 85 °C depending on the flow rate. In order to find the optimized conditions of SOAP, the effect of the optical lens array on the fluidic channels to increase the temperature of water, the change in the average temperature at the outlet with respect to the ratio of the lens diameter (D) to channel width (w) was systematically investigated. The detailed geometry of the SOAP system considered in our simulation is shown in Figures 2(b) and 2(c). The flow and temperature field are calculated by solving the Navier–Stokes (Equation (1)) and heat transfer equations (Equation (3)), assuming that the mass flow rate in a single panel, the intensity of solar radiation, and air temperature are 10^{-6} kg/s, 1000 W/m^2, and 20 °C, respectively. The widths, height, and length of the channel are 500 μm, 100 μm, and 25 mm, respectively. If we assume that our SOAP is installed on the building facade of 3 m height and 10 m width, the maximum regeneration of water would be about 4000 kg/day. In this case, our SOAP could sterilize the greywater produced by 50 inhabitants.[5] In order to concentrate the solar radiation, we chose hemispherical lens with diameters

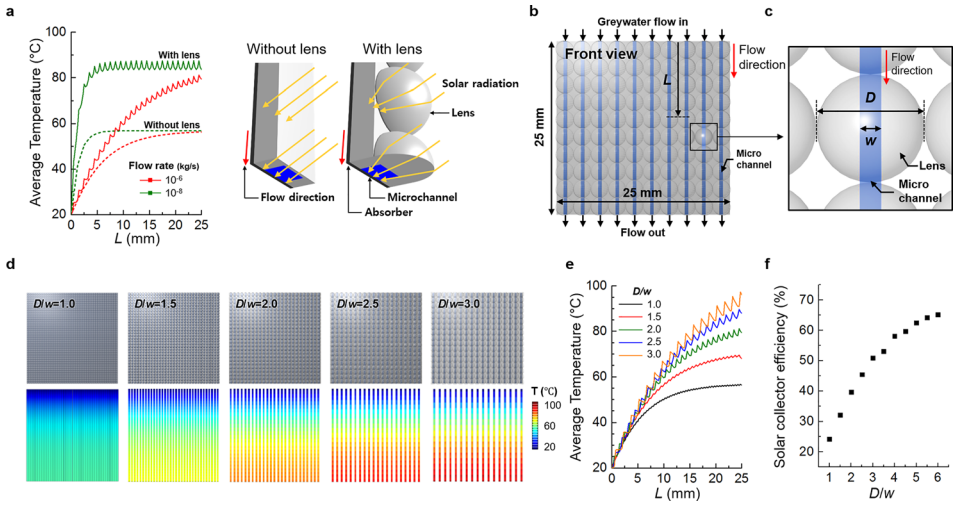

FIG. 2. The solar energy storage in SOAP: (a) Effect of optical lens array on water temperatures as a function of distance from the inlet (L) in the SOAP channel and corresponding schematic illustration of SOAP's designs (left) without optical lens and (right) with optical lens array on top of the fluidic channel. The optical lens focuses solar radiation to the microfluidic channel. (b) Detailed geometry of the SOAP system in our simulation and (c) design variables of optical lens diameter (D) and micro channel width (w) are considered in our simulation. (d) Several SOAP designs with different ratios of the lens diameter to channel width (D/w) (top row) and corresponding temperature profiles in the channels (bottom row). (e) Quantitative plot of average temperatures along the channels with respect to D/w, ranging from 1.0 to 3.0. (f) Effect of D/w on the solar collector efficiency of solar radiation. The solar collector efficiency is calculated according to the Equation (4). The mass flow rate is 10^{-6} kg/s.

ranging from 500 to 1500 μm. The refractive index of lens is set to be 2.0. The energy losses due to reflectance and absorption by the lens were assumed to be negligible in this study. Also, we assumed that heat transfer in the absorbing layer is negligible because of the low thermal conductivity of widely used absorbing materials.

Figure 2(d) shows several SOAP systems with respect to D/w and corresponding temperature profiles in the channels. The water temperature increases monotonically with respect to the increasing D/w. Figure 2(e) represents a quantitative plot of the water temperatures along the channels with respect to D/w. When the diameter of the lens increases to larger than 3.0 times the channel width, the average temperature increases by 70%, compared to that of the channel with D/w is 1.0. The gradient of the temperature with respect to D/w is gradually decreased with increasing D/w. For example, the temperature gradient when D/w is 6.0 is only 10% of the temperature gradient when D/w is 1.0.

Figure 2(f) shows the effect of D/w on the solar collector efficiency of the solar energy storage. The solar collector efficiency is defined as[26]

$$\eta = c_p \dot{m} \Delta T / G_T A, \tag{4}$$

where $\dot{m}$ is the mass flow rate in the SOAP panel, ΔT is the temperature difference between the inlet and outlet, G_T is the intensity of the solar radiation, and A is the area of the SOAP panel. The gradient of solar collector efficiency continuously decreased with increasing D/w, which is similar to the change in the water temperature at the outlet of the channel.

The installation of the optical lens on top of the SOAP channel increases the intensity of solar radiation by harnessing the solar radiation over a greater area than the area of the channels. Therefore, our SOAP design overcomes the limitation on the temperature of water in the channels without the optical lens. The systematic investigation to determine the effect of the lens diameter reveals that the temperature of water increases monotonically with respect to the increasing D/w, due to the reduction of surface area where convective heat loss occurs. The surface area of the channels is determined by D/w because the width of our SOAP panel is fixed at 25 mm for computational convenience. For example, the surface area of the channels

becomes one-half when the D/w is 2.0, compared to the surface area when the D/w is 1.0. The more solar energy that is stored in water results in the higher water temperature. However, such elevated temperature increases the temperature gradient at the channel–air interface, inducing the heat transfer to the surrounding. Consequently, the gradient of the average temperature with respect to D/w decreases gradually when the temperature of water increases according to the lens diameter.

D. Solar disinfection of pathogens in SOAP

Figure 3(a) shows a schematic image of the thermal disinfection by our SOAP channels upon solar radiation. *Escherichia coli* (*E. coli*) and *Enterococcus faecium* (*E. faecium*) are selected as representative pathogenic bacteria, since they exhibit weak and strong thermal resistance, respectively.[27] The disinfection rate (R_D) is calculated, based on thermal resistance properties of bacteria such as D_T and Z.[28–46] D_T is defined as the heat treatment time required to destroy 90% of bacteria cells at a specific temperature, T. On the other hand, Z represents the change in temperature required to increase or decrease the D_T value by 10 times. D_T is a function of temperature that can be expressed as $\log_{10}D_T = -T/Z + (\log_{10}D_{T_0} + T_0/Z)$, where D_{T_0} is the D_T value at a specific temperature, T_0, that is already given (see supplementary material Fig. S1). For example, the D_{60} and Z values of *E. coli* were reported to range from $35 \sim 42$ s to $5.9 \sim 6.1$ °C (95% confidence interval).[29–38] The D_{60} and Z values of *E. faecium* ranged from $1.0 \times 10^3 \sim 1.3 \times 10^3$ s to $8.8 \sim 11$ °C (95% confidence interval).[39–46] The effects of SOAP on water temperature and R_D with respect to lens structure (e.g., hemispherical and semi cylindrical lens) are also investigated in Figure 3(b) (see supplementary material Fig. S2). Since the

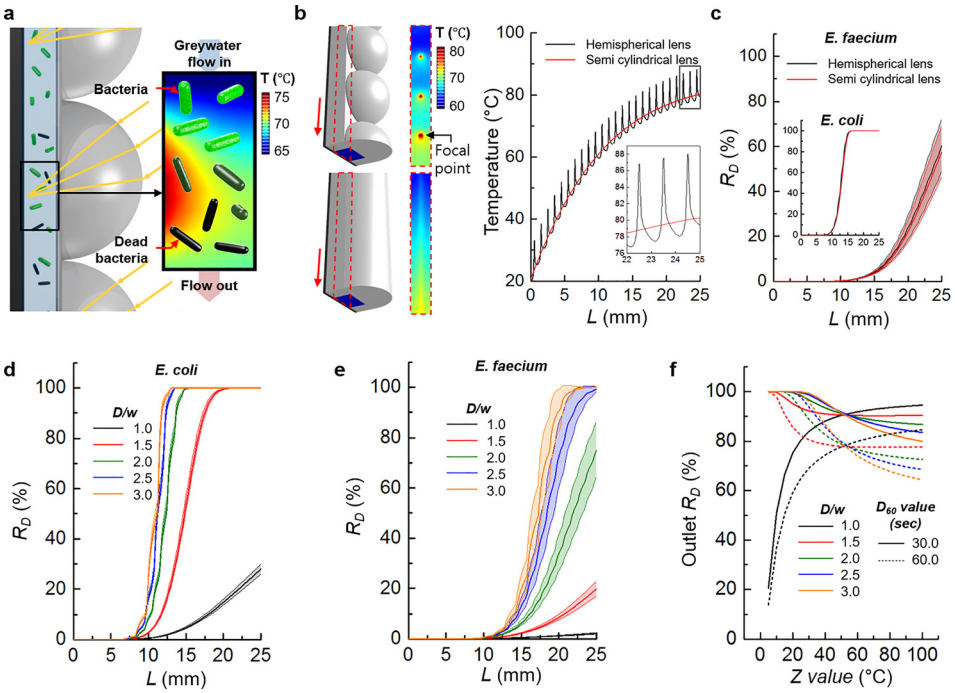

FIG. 3. Solar water disinfection of pathogens in SOAP: (a) A schematic illustration of photothermal disinfection by the solar radiation. (b) The effect of lens structures on greywater temperature in the SOAP channel as a function of L (i.e., hemispherical and semi cylindrical lens). (c) Disinfection rate (R_D) of *E. coli* and *E. faecium* as a function of L with respect to the lens structure. Band represents 95% confidence interval. Mass flow rate and D/w were set to be 1.0×10^{-6} kg/s and 2.0. R_D of (d) *E. coli* and (e) *E. faecium* as a function of L with respect to D/w of the hemispherical lens. Band represents 95% confidence interval. (f) The effect of thermal resistance properties, the D_{60} and Z values, on R_D with respect to D/w. The solid and dashed lines mean R_D as a function of Z value with respect to the 30 s and 60 s of D_{60}, respectively. The D_{60} value is defined as the heat treatment time required to destroy 90% of bacteria cells at a 60 °C. The Z value is the change in temperature required to increase or decrease the D_{60} value by 10 times.

temperature of the hemispherical lens at the focal point is higher than that of the semi cylindrical lens by about 8 °C, the hemispherical lens shows about 3% higher R_D in the case of *E. faecium* (Figure 3(c)).

The calculated disinfection rate with respect to D/w of the hemispherical lens is shown in Figures 3(d) and 3(e). When the diameter of the lens is increased to larger than 1.5 times the channel width, the disinfection rates of *E. coli* and *E. faecium* are increased by 2.0 and 7.7 times, respectively. In order to generally investigate the effect of D_T and Z values on the disinfection rate, the disinfection rate at the outlet of the channel as a function of the Z value ranging from 5 to 100 °C was simulated as shown in Figure 3(d). The D_{60} value is selected since it corresponds to the median temperature of the SOAP design from the inlet temperature (20 °C) to a boiling temperature of water (100 °C). Interestingly, the D/w ratio for better disinfection performance is changed around the Z value of 45 °C. When the Z value is less than 45 °C, large D/w is more effective for the disinfection of bacteria, since the larger D/w provides a higher temperature. On the other hand, small D/w is more effective for the disinfection of bacteria because the lower flow rate ensures a longer traveling time with the heat treatment. The disinfection rate is increased when the D_{60} value is decreased, irrespective of the D/w ratio.

E. Regional effect on solar energy storage and solar disinfection of SOAP

In order to evaluate the actual performance of the SOAP design, we investigate its potential regional effects by applying climate conditions (elevation and azimuth angles of solar radiation and air temperature) at two locations (see supplementary material Fig. S3). However, the spectral characteristics of light (i.e., wavelength) are not considered in this study. The intensity of solar radiation is calculated based on an air mass coefficient that depends on the azimuth angle and the elevation angle. The position of the focal point with respect to the incident angle of solar radiation is investigated (see supplementary material Figs. S4 and S5). Two cities, Iquique (Chile) and Phoenix (USA), are selected due as representative cases of extreme water and energy stress where research in alternative sustainable water and energy use models are under

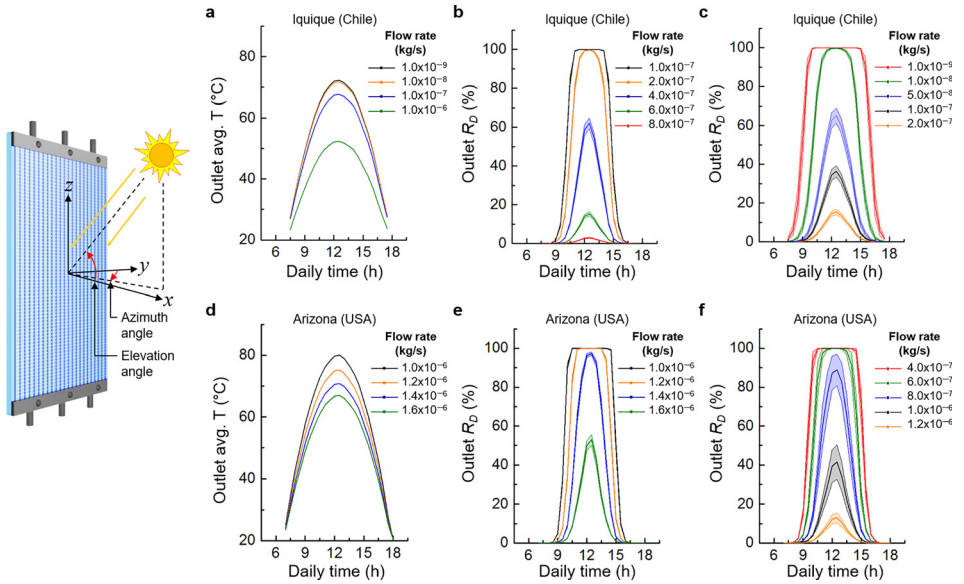

FIG. 4. Regional effect on solar energy storage and solar disinfection due to the elevation and azimuth angles of solar radiation at specific geographic locations: (a) Average outlet temperatures at the outlet of the SOAP channel under the climate conditions of Iquique. (b) Corresponding outlet disinfection rate of *E. coli* with flow rates ranging from 1.0×10^{-7} to 8.0×10^{-7} kg/s. (c) Corresponding outlet disinfection rate of *E. faecium* with flow rates ranging from 1.0×10^{-9} to 2.0×10^{-7} kg/s. (d) Average outlet temperatures at the outlet of SOAP channel under the climate conditions of Phoenix. (e) Corresponding outlet disinfection rate of *E. coli* with flow rates ranging from 1.0×10^{-6} to 1.6×10^{-6} kg/s. (f) Corresponding outlet disinfection rate of *E. faecium* with flow rates ranging from 4.0×10^{-7} to 1.2×10^{-6} kg/s. A translucent band represents 95% confidence interval.

study.[47–50] The SOAP panel is assumed to be installed on the north wall of a building in Iquique and comparatively on the south wall in Phoenix. The elevation and azimuth angles of solar radiation and air temperature are determined for autumn.

Figures 4(a) and 4(d) show the daily temperatures of water in SOAP channels in Iquique and Phoenix, respectively. Because SOAP faces toward north (Iquique) and south (Phoenix) directions, the maximum temperature of water is achieved at noon. Under the climate condition of Phoenix, the temperature of the water in the SOAP channel is 53% higher, compared to the temperature of water in Iquique. It is expected that the higher temperature in Phoenix increases the disinfection rate. The disinfection rates for *E. coli* in both cities are shown in Figures 4(b) and 4(e), respectively. The thermal disinfection of *E. coli* is found to be completed in both locations with mass flow rates ranging from 1.0×10^{-7} to 1.6×10^{-6} kg/s. However, the photothermal disinfection of *E. faecium* is insufficient with the same mass flow rates due to higher thermal resistance of *E. faecium*, as shown in Figures 4(c) and 4(f). When the mass flow rate is 1.0×10^{-6} kg/s, the disinfection rates of *E. faecium* in Iquique and Phoenix are calculated to be $0.1\% \pm 0.03\%$ and $41.6\% \pm 8.9\%$, respectively. The thermal disinfection of *E. faecium* can be completed by further decreasing the mass flow rate to 1.0×10^{-9} kg/s (Iquique) and 4.0×10^{-7} kg/s (Phoenix), respectively.

The average air temperatures in Iquique and Phoenix in autumn are 22 °C. In spite of the same air temperature in Phoenix and Iquique, the average temperature of the water in our SOAP panel is estimated to be 53% higher than that of the water in Iquique. This can be attributed to the elevation angle of solar radiation at two locations. Due to the lower elevation angle, the intensity of solar radiation in Phoenix can be higher by up to 81% than that in Iquique.

III. CONCLUSIONS

In summary, we have demonstrated an effective design of SOAP as a *lab-on-a-wall*, which allows a holistic integration of energy generation and water regeneration. Our SOAP *lab-on-a-wall* has dual functions of solar energy storage and photothermal disinfection of bacteria. The optical lens on top of the SOAP microfluidic channel can focus the solar radiation over a greater area than the area of the channels. As a result, the water temperature can be significantly increased by 70% when the ratio of the lens diameter to the channel width is increased by up to 3.0 times, compared to the channel without the lens. In addition, our SOAP can accomplish 100% disinfection rate for pathogens, such as *Escherichia coli*. Geographic locations are found to be also critical on solar energy storage and solar disinfection of SOAP, which is very useful in the determination of locale for the incorporation of SOAP into a building facade in a given urban context and region (e.g., the orientation of SOAP on the building facade). Multiscale design and analysis of SOAP for sustainable building can mark a new era for resourcing resources in future smart city and building science, where solutions of water, energy, and waste problems can be synergistically resolved.

SUPPLEMENTARY MATERIAL

See supplementary material for the numerical and analytical details, effects of lens structure, facade orientation, and incident angle of the solar radiation.

ACKNOWLEDGMENTS

We are grateful for the support of the National Science Foundation (EFRI-SEED Grant Award No. 1038279), Korea CCS R&D Center (KCRC) (Grant No. 2015M1A8A1053539), International Research & Development Program (Grant No. 2013K1A3A1A32035444), Mid-Career Researcher Support Program (Grant Nos. 2014R1A2A2A09052374 and 2016R1A2B3014157), and C1 Gas Refinery Program (Grant No. 2016M3D3A1A01913546) of the National Research Foundation of Korea (NRF) funded by the Ministry of Science, ICT & Future Planning, Korea.

[1]K. G. Satyanarayana, A. B. Mariano, and J. V. C. Vargas, Int. J. Energy Res. **35**, 291–311 (2011).
[2]A. Demirbas, Energy Sources, Part B **4**, 212–224 (2009).
[3]C. Nellemann and B. P. Kaltenborn, ICIMOD (2009), Vol. 56, pp. 6–9.

[4]R. Penn, M. Hadari, and E. Friedler, Urban Water J. **9**, 137–148 (2012).
[5]G. Antonopoulou, A. Kirkou, and A. S. Stasinakis, Sci. Total Environ. **454**, 426–432 (2013).
[6]T. M. Joyce, K. G. McGuigan, M. Elmore-Meegan, and R. M. Conroy, Appl. Environ. Microbiol. **62**, 399–402 (1996).
[7]K. G. Lindenauer and J. L. Darby, Water Res. **28**, 805–817 (1994).
[8]K. G. McGuigan, R. M. Conroy, H. J. Mosler, M. du Preez, E. Ubomba-Jaswa, and P. Fernandez-Ibanez, J. Hazard. Mater. **235**, 29–46 (2012).
[9]B. Sommer, A. Marino, Y. Solarte, M. L. Salas, C. Dierolf, C. Valiente, D. Mora, R. Rechsteiner, P. Setter, and W. Wirojanagud, J. Water Supply Res. T. **46**, 127–137 (1997).
[10]H. C. Hottel and T. A. Unger, Sol. Energy **3**, 10–15 (1959).
[11]M. G. Hutchins, P. J. Wright, and P. D. Grebenik, Sol. Energy Mater. **16**, 113–131 (1987).
[12]J. E. Minardi and H. N. Chuang, Sol. Energy **17**, 179–183 (1975).
[13]T. P. Otanicar, P. E. Phelan, R. S. Prasher, G. Rosengarten, and R. A. Taylor, J. Renewable Sustainable Energy **2**, 033102 (2010).
[14]H. Tyagi, P. Phelan, and R. Prasher, J. Sol. Energy Eng. **131**, 041004 (2009).
[15]D. Y. Goswami and F. Kreith, *Handbook of Energy Efficiency and Renewable Energy* (CRC Press, Florida, 2007).
[16]C. J. Winter, R. L. Sizmann, and L. L. Vant-Hull, *Solar Power Plants: Fundamentals, Technology, Systems, Economics* (Springer Science & Business Media, New York, 2012).
[17]D. Mills, Sol. Energy **76**, 19–31 (2004).
[18]A. K. Athienitis, Sol. Energy **61**, 337–345 (1997).
[19]H. J. Bullinger and L. Behlau, *Technology Guide: Principles-Applications-Trends* (Springer, New York, 2009).
[20]ASHRAE, ASHRAE Vision 2020, see www.ashrae.org/File%20Library/docLib/Public/20080226_ashraevision2020.pdf (2008) (last accessed April 3, 2016).
[21]D. Crawley, S. D. Pless, and P. A. Torcellini, *Getting to Net Zero* (National Renewable Energy Laboratory, 2009).
[22]I. Sartori, A. Napolitano, and K. Voss, Energy Build. **48**, 220–232 (2012).
[23]S. Attia, M. Hamdy, W. O'Brien, and S. Carlucci, Energy Build. **60**, 110–124 (2013).
[24]OECD, "Design of sustainable building policies: Scope for improvement and barriers," see www.oecd.org/officialdocuments/publicdisplaydocumentpdf/?doclanguage=en&cote=env/epoc/wpnep(2001)5/final (2002) (last accessed April 3, 2016).
[25]M. P. Gutierrez and L. P. Lee, Science **341**, 247–248 (2013).
[26]J. A. Duffie and W. A. Beckman, *Solar Engineering of Thermal Processes* (John Wiley & Sons, New York, 2013).
[27]S. Sorqvist, Acta Vet. Scand. **44**, 1–20 (2003).
[28]C. R. Stumbo, *Thermo-Bacteriology in Food Processing*, 2nd ed. (Academic Press, New York, 1973).
[29]R. B. Read, Jr., N. L. Norcross, D. J. Hankinson, and W. Litsky, J. Dairy Sci. **40**, 28–36 (1957).
[30]R. M. Lemcke and H. R. White, J. Appl. Bacteriol. **22**, 193–201 (1959).
[31]R. B. Read, Jr., C. Schwartz, and W. Litsky, Appl. Microbiol. **9**, 415–418 (1961).
[32]C. L. Calhoun and W. C. Frazier, Appl. Microbiol. **14**, 416–420 (1966).
[33]D. A. Evans, D. J. Hankinson, and W. Litsky, J. Dairy Sci. **53**, 1659–1665 (1970).
[34]J. M. Goepfert, I. K. Iskander, and C. H. Amundson, Appl. Microbiol. **19**, 429–433 (1970).
[35]R. Dabbah, W. A. Moats, and V. M. Edwards, J. Dairy Sci. **54**, 1772–1779 (1971).
[36]C. A. Dega, J. M. Goepfert, and C. H. Amundson, Appl. Microbiol. **23**, 415–420 (1972).
[37]N. Katsui, T. Tsuchido, M. Takano, and I. Shibasaki, J. Gen. Microbiol. **122**, 357–361 (1981).
[38]M. Ahmad, B. S. Srivastava, and S. C. Agarwala, J. Gen. Microbiol. **107**, 37–44 (1978).
[39]C. A. Magnus, A. R. McCurdy, and W. M. Ingledew, Can. Inst. Food Sci. Technol. J. **21**, 209–212 (1988).
[40]C. A. Magnus, A. R. McCurdy, and W. M. Ingledew, J. Food Prot. **51**, 895–897 (1988).
[41]S. Quintavalla and S. Barbuti, Ind. Conserve **64**, 8–12 (1989).
[42]C. A. Gordon and M. H. Ahmad, Can. J. Microbiol. **37**, 609–612 (1991).
[43]J. L. Kornacki and E. H. Marth, Milchwissenschaft (Germany) **47**, 764–769 (1992).
[44]S. S. Patel and R. A. Wilbey, J. Dairy Res. **61**, 263–270 (1994).
[45]M. V. Simpson, J. P. Smith, H. S. Ramaswamy, B. K. Simpson, and S. Ghazala, Food Res. Int. **27**, 349–353 (1994).
[46]A. M. Kearns, R. Freeman, and N. F. Lightfoot, J. Hosp. Infect. **30**, 193–199 (1995).
[47]L. A. Baker, A. J. Brazel, N. Selover, C. Martin, N, McIntyre, F. R. Steiner, A. Nelson, and L. Musacchio, Urban Ecosyst. **6**, 183–203 (2002).
[48]S. Guhathakurta and P. Gober, J. Am. Plann. Assoc. **73**, 317–329 (2007).
[49]R. E. Dixon, Desalin. Water Treat. **51**, 5–10 (2013).
[50]E. A. Wentz and P. Gober, Water Resour. Manage. **21**, 1849–1863 (2007).